Image-Guided Spatial Localization of Heterogeneous Compartments by Compressed Sensing

Li An[1] and Jun Shen[1]

[1]*National Institute of Mental Health, National Institutes of Health, Bethesda, MD, United States*

Target audience: Scientists and clinicians who want to efficiently obtain spectra from anatomical regions with natural and irregularly shaped boundaries.

Purpose: Image-guided localization method such as SLIM (Spectral Localization by IMaging) (1) and SPLASH (SPectral Localization Achieved by Sensitivity Heterogeneity) (2) allow extraction of signals from irregularly shaped anatomical compartments. Here, we propose a novel method to take into consideration of biologically inhomogeneous signal distribution within each compartment. We first subdivide each compartment into multiple smaller subcompartments to capture intra-compartment heterogeneous signal distribution and then use compressed sensing for regularization. Application of this new method to single-shot separation of MRS signals from stroke and normal tissue compartments is demonstrated.

Methods:

Generation of subcompartments: A software program was developed (2) to display anatomical images with the option of overlaying the MRS volume of interest (VOI) box on them (see Fig. 2). It also allowed the user to manually draw polylines to define compartment boundaries and to pick a few image pixels, one in each compartment, to be used as initial seed points for a region growing process. In the region growing process, each compartment was grown separately starting from one initial seed point and stopping at the boundaries defined by the VOI box and the user-drawn polylines. After this process, the VOI was partitioned into a few compartments defined by the user-drawn boundaries. To allow intracompartment variations, the user-defined compartments were automatically partitioned into smaller subcompartments. First, the whole VOI was divided uniformly into rectangular shaped voxels whose size was comparable to that of proton chemical shift imaging. The voxels that were located entirely in one compartment were directly assigned as subcompartments. Some voxels lay on the compartment boundaries and thus were split into multiple fractions by the compartment boundaries. These voxel fractions were fused with a neighboring voxel or voxel fractions in the same compartment.

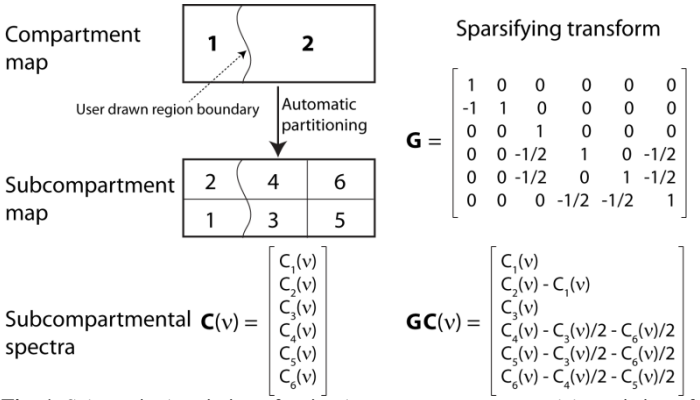

Fig. 1. Schematic description of a simple two-compartment model consisting of six-subcompartments.

Solving for the subcompartmental spectra: The equations for computing subcompartmental spectra from multichannel data collected without phase encoding gradients are briefly described here. In the frequency domain, spectrum $D_m(\nu)$ which is the Fourier transform of the time domain signal received by the mth coil element can be expressed as $D_m(\nu) = \sum_{n=1}^{N} S_{m,n} C_n(\nu) + \varepsilon_m(\nu)$, for $m = 1, 2,\ldots, M$ [1], where N is the total number of subcompartments and M the total number of coil elements or signal channels; $C_n(\nu)$ is the spectrum of the nth subcompartment; $\varepsilon_m(\nu)$ is the random noise in the mth channel; and $S_{m,n}$ is the integrated sensitivity of the mth coil element over the nth subcompartment: $S_{m,n} = \int_{\text{compartment } n} s_m(\boldsymbol{r}) d^3\boldsymbol{r}$, with $s_m(\boldsymbol{r})$ being the sensitivity of the mth coil element at location $\boldsymbol{r}$. For each frequency ν, Eq. [1] can be expressed in matrix form as $\boldsymbol{D}=\boldsymbol{SC}+\boldsymbol{\varepsilon}$ [2]. The noise covariance matrix $\boldsymbol{\Psi}$, defined as $E[\boldsymbol{\varepsilon\varepsilon}^{\dagger}]$, can be eigendecomposed into $\boldsymbol{\Psi}=\boldsymbol{U\Lambda U}^{\dagger}$. After moving $\boldsymbol{SC}$ to the left side of Eq. [2] and multiplying the noise whitening matrix $\boldsymbol{\Lambda}^{-1/2}\boldsymbol{U}^{\dagger}$ to both side of Eq. [2], we have: $\boldsymbol{\Lambda}^{-1/2}\boldsymbol{U}^{\dagger}(\boldsymbol{D}-\boldsymbol{SC})=\boldsymbol{\Lambda}^{-1/2}\boldsymbol{U}^{\dagger}\boldsymbol{\varepsilon}$ [3]. Vector $\boldsymbol{C}$ can be solved by minimizing the sum of the L2-norm of $\boldsymbol{\Lambda}^{-1/2}\boldsymbol{U}^{\dagger}(\boldsymbol{D}-\boldsymbol{SC})$ and a L1 regularization term $\lambda\|\boldsymbol{GC}\|$: minimize $\|\boldsymbol{\Lambda}^{-1/2}\boldsymbol{U}^{\dagger}(\boldsymbol{D}-\boldsymbol{SG}^{-1}\boldsymbol{GC})\|^2+\lambda\|\boldsymbol{GC}\|$ [4], where an $N\times N$ identity matrix $\boldsymbol{G}^{-1}\boldsymbol{G}$ is inserted between $\boldsymbol{S}$ and $\boldsymbol{C}$. Vector $\boldsymbol{GC}$ represents the differences between each subcompartment and its neighboring subcompartments in the same full compartment except that the first subcompartment in each full compartment is preserved to make $\boldsymbol{G}$ invertible. The construction of the sparsifying matrix $\boldsymbol{G}$ is illustrated in Fig. 1. Let $\boldsymbol{Y}=\boldsymbol{\Lambda}^{-1/2}\boldsymbol{U}^{\dagger}\boldsymbol{D}$, $\boldsymbol{A}=\boldsymbol{\Lambda}^{-1/2}\boldsymbol{U}^{\dagger}\boldsymbol{SG}^{-1}$, and $\boldsymbol{X}=\boldsymbol{GC}$, Eq. [4] is transformed into: minimize $\|\boldsymbol{Y}-\boldsymbol{AX}\|^2+\lambda\|\boldsymbol{X}\|$ [5], which is a standard L1 regularized least square problem and can be solved, point-by-point in the frequency domain, using compressed sensing algorithms (3). After $\boldsymbol{X}$ is obtained, multiplying $\boldsymbol{G}^{-1}$ to $\boldsymbol{X}$ yields the desired subcompartmental spectra $\boldsymbol{C}$. The average of all subcompartmental spectra in a compartment weighted by the volume of each subcompartment was taken as the spectrum for that compartment.

In vivo experiments: Compartmental spectra were reconstructed using both the original SPLASH method and the L1 regularization method from the *in vivo* CSI data of a stroke patient (2). To illustrate the effectiveness of L1 regularized SPLASH compartmental localization, only the dc-components of the chemical shift imaging (CSI) data (i.e., $k_x = k_y = 0$) were used for reconstruction. The effective scan time was 4 s (TR = 2 with two averages).

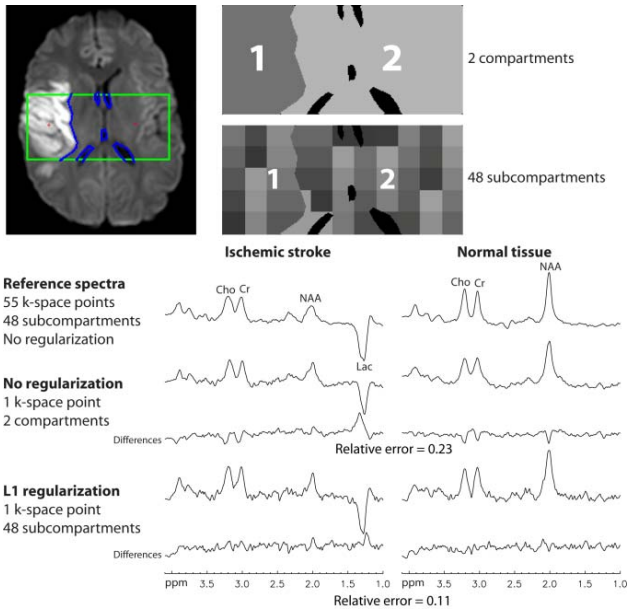

Fig. 2 Compartmental spectra computed using data from a stroke patient. The MRS pulse sequence used TR = 2 s, TE = 144 ms, volume of interest (VOI) = 110 × 50 × 14 mm^3, phase encoding matrix = 11 × 5, number of signal averages = 2. A diffusion weighted imaging (DWI) image of the patient is displayed on top, along with the volume of interest (VOI; green box), user-drawn compartment boundaries (blue polyline), and two initial seed points for region growing (red dots). Compartment and subcompartment maps generated by region growing are displayed beside the DWI image, where different grey levels are used to differentiate different compartments. The top compartmental spectra, which were computed using all 11 × 5 k-space data, were used as the reference spectra. The bottom two sets of compartmental spectra were reconstructed from the dc-component of the k-space data using the original SPLASH and the L1 regularization method.

Results: Reconstructed compartmental spectra are displayed in Fig. 2. The two compartmental spectra for the original SPLASH method were very different from the reference spectra at the positions of all four metabolite peaks. The L1 regularization method significantly reduced the differences at the NAA, Cr, and Cho peaks. The estimated relative error was reduced from 0.23 to 0.11 after L1 regularization.

Discussion and Conclusion: An L1 regularization method for SPLASH was proposed to allow reconstruction of compartmental spectra from irregularly shaped compartments with heterogeneous distribution of metabolite concentrations. Compartmental spectra reconstructed from *in vivo* CSI data demonstrated that the L1 regularization method significantly reduced metabolite quantification errors. Although the proposed method was demonstrated using MRS, it serves as a general spatial localization method and can be used to measure other tissue properties from irregularly shaped compartments with heterogeneous signal distribution.

References: 1. Hu XP, *et al.*, MRM 1988;8 (3): 314-322. 2. An. L, *et al.*, MRM 2011;66(1):1-10. 3. Kim SJ, *et al.*, IEEE STSP 2007;1(4):606-617.